International Journal of Science Academic Research
Vol. 06, Issue 06, pp.10193-10201, June, 2025
Available online at http://www.scienceijsar.com

ISSN: 2582-6425

Research Article

AN INVESTIGATION ON VERTICAL PERMEABLE CHANNEL UNDER RADIATIVE MHD FLOW OF NANOFLUID

***Shyam Manohar Suthar and Shweta Bohra**

Department of Mathematics, Sangam University, Bhilwara, Rajasthan 311011, India

Received 18th April 2025; **Accepted** 24th May 2025; **Published online** 20th June 2025

Abstract

Free convective Magneto hydrodynamics (MHD) Couette flow of nanofluid through a porous medium in a vertical permeable channel with thermal radiation and suction/injection. A Cu-ethylene glycol nanofluid is evaluated. The class of equations and their numerical integration are discretized by means of C.N. (Crank-Nicolson) implicit difference scheme for the integrated governing unsteady mass, momentum & energy equation systems. In the present article, the steady-state fluid flow with heat transfer have been studied by this mathematical model. Hence, the analysis and comparison of the steady and the unsteady are presented. The dominance of various physical parameters are displayed in the form of graphs for velocity and temperature profiles for both cases.

Keywords: MHD Flow, Nanofluid, Thermal Radiation, Crank-Nicolson implicit difference.

INTRODUCTION

The region of free natural convection, whether in vertical or horizontal channels, has some technical use. An industrial or engineering application will always have channel flow. Most modern materials processing has to do with free convection MHD flows with radiation because so many researchers are tired of studying flow. Kumar *et al.* [1] observed the natural convective flow in two regions. They were in a vertical channel, the lower one was filled with a micropolar fluid and the upper one was viscous. In the study of the effects of inertial force in mixed convection flow between vertical channels of porous medium, Umavathi *et al.* [2] considered the effects of Darcy and Viscous dissipation. Unsteady MHD conjugate flow for different fluids over an oscillating vertical plate contained in a porous medium has been done by Hussanam et al.[3] and Khalid et al.[4]. Khem *et al.* [5]analyzed MHD Couette flow of a viscous incompressible electrically conducting fluid through completely porous medium bounded laterally by two insulated vertical porous plates. The problem of transient natural convection Couette flow between two infinite vertical parallel plates has been solved by Jha *et al.* [6], [7]. The effects of radiation, chemical reaction, Soret, and heat generation effects on MHD free convective Casson fluid flow past an oscillating vertical have been studied by Kataria and Patel [8], [9]. Various physical processes of engineering which employ suction/injection such as skin cooling, removal of reactants, prevention of corrosion, thermal oil recovery, and thrust-bearing design applications have made unsteady MHD free-convection flow a burning topic today. Operations in flow alike Couette-Flow and transfer of heat with suction/injection effects on varying properties have been analyzed by Attia [10]. The fluid flow effects of both injection & suction under the unsteady conditions of two parallel plates in a permeable media were examined by Makinde and Rundora [11] under convective boundary conditions and using a third-grade fluid model with viscosity as variable. Jha *et al.* [12], [13] have shown both the analytical and numerical solution for Couette flow of incompressible viscous fluids between two-infinite vertical porous plates and vertical channels respectively. Research has been done in other areas, revealing the performances of heat transfer in fluids with the addition of particles as early as Maxwell first proposed it. The researchers, Choi and Eastman, introduced the concept of 'Nanofluids' whereby ultrafine nanoparticles are suspended in a base fluid to counteract many problems due to large suspended particles, including quick sedimentation and blocking of channels. Buddakkagari and Kumar studied the hydrodynamic transient boundary layer flow of nanofluids over a flat cone and plate with constant boundary conditions using the Crank Nicolson implicit difference method, which was followed by Chouhan and Kumar to examine the effect of radiation and unsteady flow over velocity and temperature slip boundary conditions in a porous medium channel. However, based on the past studies in many researchers' efforts, numerous works have been investigated concerning numerical simulation of convective boundary heat transfer of nanofluids in vertical plates or channels while accounting for a series of effects like under magneto hydrodynamics and radiation as indicated in references [14], [15], [16], [17], [18], [19], [20], [21], [22], [23], [24], [25], [26], [27], [28], [29]. Additionally, there are the studies on mixed convective magnetohydrodynamic water-based nanofluids in a variety of geometries such as vertical channels, stretching sheets, inclined ducts, cylinders, inclined cylinders, and wavy channels in the indices of references [30], [31], [32], [33], [34], [35], [36], [37]. The present research attempts to study free convective magneto hydrodynamic Couette flow of nanofluid in a vertical porous channel whose boundaries are subjected to thermal radiation effects, suction, and injection into the porous medium. Steady-state and unsteady flow under the same boundary conditions is analyzed for heat transfer characteristics. The results also coincide with recent literature.

Corresponding Author:** ***Shyam Manohar Suthar
Department of Mathematics, Sangam University, Bhilwara, Rajasthan 311011, India

MATHEMATICAL FORMULATION

This present study deliberates over the unsteady free convective Couette flow occurring between the two infinite porous plates under the influence of a B_0 (transverse magnetic field) along with the q_r(radiation of intensity) in a vertical channel.

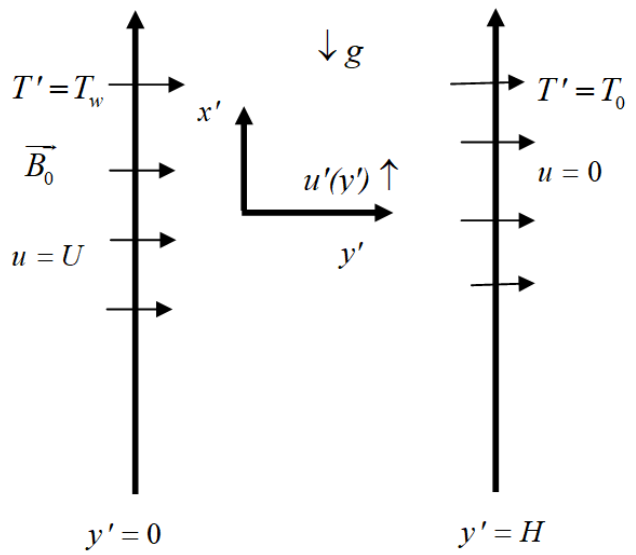

Fig. 1. Physical configuration and coordinate system

The fluid motion-induced induced magnetic field is assumed to be small compared to the externally applied magnetic field, that is, magnetic Reynolds number very small. In addition, Ohmic heating, ion slip, and Hall effects are neglected concerning them having a very insignificant effect on the matter concerned. The study is based on copper nanoparticles suspended in Ethylene glycol, with the nanoparticles being spherical and uniformly sized and remaining in thermal equilibrium with the base fluid. We set up x', y' (rectangular Cartesian coordinate system) wherein the x'-axis is directed along the vertical plate which moving in the upward direction and the y'-axis is taken to be normal to the plane of the plate. Since the porous plates are assumed to be infinite, the velocity and time thus depend only on y' and t'. The fluid and the permeable plates inside the channel are at rest at time $t' = 0$, and the system is at uniform temperature T_0. At $y' = 0$, a porous plate begins to move in the x' direction with velocity U, for $t' > 0$, while at the same time setting the surface temperature of the plate to T_w. The other porous plate is kept at a distance H from the moving plate at a constant temperature T_0 (with $T_w > T_0$). Suction/injection at velocity V_0 is assumed for the moving porous plate located at $y' = 0$.

The governing momentum & energy equations in dimensional form are:

$$\rho_{nf}\left[\frac{\partial u'}{\partial t'} + V_0\frac{\partial u'}{\partial y'}\right] = \mu_{nf}\frac{\partial^2 u'}{\partial y'^2} - \sigma B_0^2 u' + (\rho\beta)_{nf}\, g(T' - T_0) - \frac{\mu_{nf}}{k_0}u \quad (1)$$

$$\left(\rho C_p\right)_{nf}\left[\frac{\partial T'}{\partial t'} + V_0\frac{\partial T'}{\partial y'}\right] = k_{nf}\frac{\partial^2 T'}{\partial y'^2} - \frac{\partial q_r}{\partial y'} \quad (2)$$

Appropriate boundary conditions are

$$t' \le 0: u' = 0, T' = T_0, 0 \le y \le H$$

$$t' \ge 0: \begin{cases} u' = U, T' = T_w\,, at\ y' = 0 \\ u' = 0, T' = T_0\,,\ at\ y' = H \end{cases} \quad (3)$$

$$\mu_{nf} = \frac{\mu_f}{(1-\phi)^{2.5}}\,,\ \rho_{nf} = (1-\phi)\rho_f + \phi\rho_s\,,$$

$$\nu_{nf} = \frac{\mu_{nf}}{\rho_{nf}}\,,\ (\rho\beta)_{nf} = (1-\phi)(\rho\beta)_f + \phi(\rho\beta)_s\,,$$

$$\frac{k_{nf}}{k_f} = \frac{(k_s+(n-1)k_f) - \phi(n-1)(k_f - k_s)}{(k_s+(n-1)k_f) + \phi(k_f - k_s)}\,,$$

$$\left(\rho C_p\right)_{nf} = (1-\phi)\left(\rho C_p\right)_f + \phi\left(\rho C_p\right)_s \quad (4)$$

To measure k_{nf} (thermal conductivity) of the nanofluid for different shapes of nano particles, we adopted the following formula which is discovered by Hamilton and Crosser [30]. Here n is the nano particle shape, for spherical $n = 3$ and for cylindrical shaped particles $n = \frac{3}{2}$. In this discussion, we have considered spherical nanoparticles.

for radiation effect we use Rosseland diffusion approximation:

$$q_r = -\frac{4\sigma_1}{3k_1}\frac{\partial T'^4}{\partial y'}$$

We considered the temperature differences in the flow such that the term T^4 can actually be approximated to a linear function in temperature. This can be done by Taylor expanding T^4 about T_0, dropping all second and higher-order terms:

$$T^4 \cong 4T_0^3 T' - 3T_0^4$$

$$\frac{\partial q_r}{\partial y'} = \frac{\partial}{\partial y'}\left(-\frac{4\sigma_1}{3k_1}\frac{\partial T'^4}{\partial y'}\right) = \frac{\partial}{\partial y'}\left(-\frac{4\sigma_1}{3k_1}\frac{\partial\left(4T_0^3 T' - 3T_0^4\right)}{\partial y'}\right) = \frac{-16\sigma_1 T_0^3}{3k_1}\frac{\partial^2 T'}{\partial y'^2} \quad (5)$$

The Table 1 shows the physical properties of Cu particles and the base liquid $(CH_2\ OH)_2$ (ethylene glycol).

Table1.Thermo-physicalpropertiesoffluid f&nanoparticles [24]

Physical properties	EthyleneGlycol	Cu(Copper)
$\boldsymbol{Cp}$(J/kgK)	2415	385
$\boldsymbol{\rho}$(kg/m3)	1114	8933
$\boldsymbol{k}$ (W/mK)	0.252	400
β(1/K)	57×10^{-5}	1.67×10^{-5}

The dimensionless quantities that convert the present problem into the dimensionless form are:

$$t = \frac{t'\nu_{nf}}{H^2}\,,\ y = \frac{y'}{H}\,,\ u = \frac{u'}{U}\,,\ \theta = \frac{T'-T_0}{T_w-T_0}\,.$$

Where:

$$M^2 = \frac{\sigma B_0^2 H^2}{\rho_f \nu_f}\,,\ Pr = \frac{k_f}{(\nu\rho C_p)_f}\,,\ S = \frac{V_0 H}{\nu_f}\,,\ Gr = \frac{g\beta_f H^2(T_w - T_0)}{U\nu_f}\,,$$

$$N = \frac{4\sigma_1 T_0^3}{k_1 k_f}\,,\ K = \frac{k_0}{H^2} \quad (6)$$

Using equations (4-6) in equations (1-3), we get the non-dimensional form of momentum & energy equations with their respective boundary conditions, respectively:

$$\phi_1\phi_2\frac{\partial u}{\partial t} + S\frac{\partial u}{\partial y} = \frac{\partial^2 u}{\partial y^2} + Gr\phi_1\phi_3\theta - \phi_1 M^2 u - \frac{u}{K} \quad (7)$$

$$Pr\phi_4\left[\frac{\partial\theta}{\partial t} + S\,\frac{\partial\theta}{\partial y}\right] = \left(\frac{k_{nf}}{k_f} + \frac{4N}{3}\right)\frac{\partial^2\theta}{\partial y^2} \quad (8)$$

With the dimensionless initial & boundary conditions as:

$$t \le 0 : u = 0, \theta = 0, 0 \le y \le 1$$
$$t \ge 0 : \begin{cases} u = 1, \theta = 1, at\ y = 0 \\ u = 0, \theta = 0, at\ y = 1 \end{cases} \quad (9)$$

Where:

$\phi_1 = (1-\phi)^{2.5}, \phi_2 = 1 - \phi + \phi\left(\frac{\rho_s}{\rho_f}\right), \phi_3 = 1 - \phi + \phi\frac{(\rho\beta)_s}{(\rho\beta)_f}, \phi = 1 - \phi + \phi\frac{(\rho C_p)_s}{(\rho C_p)_f}$.

METHOD OF SOLUTION

For the transient, nonlinear momentum, and energy equations (7) and (8), subject to their initial and boundary conditions by (9), the Crank-Nicolson implicit finite difference scheme has been adopted. It is extensively used in several problems of partial differential equations and is generally regarded as reliable. All time steps anyway must be stable with respect to the spatial grid sizes. The method adopts a central difference scheme in space while treating time implicitly. Constructed and solved using the tridiagonal matrix algorithm, the difference equations represent partial differential elements of the equations. The trapezoidal rule is applied for the transient problems, giving the method second-order convergence. The Crank-Nicolson method (CNM) has been effectively implemented under various boundary conditions for conduction, radiation, and convection flow. The computational domain $(0 < t < \infty)\&(0 < y < 1)$ is divided into a mesh of lines parallel to the t and y axis.

We list the FDE (finite difference equations) that correspond to Equations (7) & (8).

$$\phi_1\phi_2\left[\frac{u_{i,j+1}-u_{i,j}}{\Delta t}\right] + S\phi_1\phi_2\left[\frac{u_{i+1,j+1}-u_{i,j+1}+u_{i+1,j}-u_{i,j}}{2\Delta y}\right] = \left[\frac{u_{i-1,j+1}-2u_{i,j+1}+u_{i+1,j+1}+u_{i-1,j}-2u_{i,j}+u_{i+1,j}}{2(\Delta y)^2}\right] + Gr\phi_1\phi_3\left[\frac{\theta_{i,j+1}+\theta_{i,j}}{2}\right] - \left(\phi_1 M^2 + \frac{1}{K}\right)\left[\frac{u_{i,j+1}+u_{i,j}}{2}\right] \quad (10)$$

$$Pr\,\phi_4\left[\frac{\theta_{i,j+1}-\theta_{i,j}}{\Delta t}\right] + Pr\,S\,\phi_4\left[\frac{\theta_{i+1,j+1}-\theta_{i,j+1}+\theta_{i+1,j}-\theta_{i,j}}{2\Delta y}\right] = \left(\frac{k_{nf}}{k_f}+\frac{4N}{3}\right)\left[\frac{\theta_{i-1,j+1}-2\theta_{i,j+1}+\theta_{i+1,j+1}+\theta_{i-1,j}-2\theta_{i,j}+\theta_{i+1,j}}{2(\Delta y)^2}\right] \quad (11)$$

Here, along the y- axis grid point classifies by the subscript i, j along the t-direction. For calculation step sizes an appropriate mesh size is considered as $\Delta t = 0.001$and $\Delta y = 0.01$ for t and y, respectively. From the initialconditions the values of u and θ are known at all grid points at $t = 0$. The known data from the previous time step (j) are used for calculating u and θ at time level $j+1$.

The equation (10)-(11) (finite difference equations)are transformed to the following algebraic equations:

$$u_{i+1,j+1}[\phi_1\phi_2 S\lambda\Delta y - \lambda] + u_{i,j+1}\left[2\phi_1\phi_2 - \phi_1\phi_2 S\lambda\Delta y + 2\lambda + \Delta t\phi_1 M^2 + \frac{\Delta t}{K}\right] - \lambda u_{i-1,j+1} =$$

$$u_{i+1,j}[\lambda - \phi_1\phi_2 S\lambda\Delta y] + u_{i,j}\left[2\phi_1\phi_2 + \phi_1\phi_2 S\lambda\Delta y - 2\lambda - \Delta t\phi_1 M^2 - \frac{\Delta t}{K}\right] + \lambda u_{i-1,j} + S_{i,j} \quad (12)$$

$$\theta_{i+1,j+1}\left[Pr\,\phi_4 S\lambda\Delta y - \left(\frac{k_{nf}}{k_f}+\frac{4N}{3}\right)\lambda\right] + \theta_{i,j+1}\left[2\,Pr\,\phi_4 - Pr\,\phi_4 S\lambda\Delta y + 2\left(\frac{k_{nf}}{k_f}+\frac{4N}{3}\right)\lambda\right] - \left(\frac{k_{nf}}{k_f}+\frac{4N}{3}\right)\lambda\theta_{i-1,j+1} = \theta_{i+1,j}\left[\left(\frac{k_{nf}}{k_f}+\frac{4N}{3}\right)\lambda - Pr\,\phi_4 S\lambda\Delta y\right] + \theta_{i,j}\left[2\,Pr\,\phi_4 + Pr\,\phi_4 S\lambda\Delta y - 2\left(\frac{k_{nf}}{k_f}+\frac{4N}{3}\right)\lambda\right] + \left(\frac{k_{nf}}{k_f}+\frac{4N}{3}\right)\lambda\theta_{i-1,j} \quad (13)$$

Where$\lambda = \frac{\Delta t}{(\Delta y)^2}$ and $S_{i,j} = \Delta t Gr\phi_1\phi_2(\theta_{i,j+1} + \theta_{i,j})$ under the initial & boundary conditions

$$u_{i,j} = 0, \quad i = 1,2,\ldots\ldots,q+1,$$
$$\left.\begin{matrix} u_{1,j} = 1 \\ u_{q+1,j} = 0 \end{matrix}\right\} \quad j = 2,3,\ldots\ldots,p+1, \quad (14)$$
$$\theta_{i,j} = 0, \quad i = 1,2,\ldots\ldots,q+1,$$
$$\left.\begin{matrix} \theta_{1,j} = 1 \\ \theta_{q+1,j} = 0 \end{matrix}\right\} \quad j = 2,3,\ldots\ldots,p+1. \quad (15)$$

Let the finite difference equation (8) be a tri-diagonal system of equations at every internal nodal point on a fixed i-level. Such a system of equations is solved by the algorithm described by Thomas. Thus, the values of θ are found for all nodal points on a particular i at the time level $(j+1)$. Similarly, the values of u are computed first from equation (8). Hence, u and θ are known at a particular i-level. The above is then repeated for the different i levels. The values of u and θ are thus known at all grid points in the rectangular region at the $(j+1)$ time level. The computations will continue until a steady state is reached. It is assumed that those conditions in steady states have been achieved when, at all grid points, the absolute differences for velocity u and temperature θ between values for two consecutive time features are less than 10^{-5}.

Particular Case: Steady state

In other words, we converted to steady state the present problem and solved it analytically. The equations in steady states with boundary conditions are:

$$\frac{d^2u}{dy^2} - S\phi_1\phi_2\frac{du}{dy} - \left(\phi_1 M^2 + \frac{1}{K}\right)u = -Gr\phi_1\phi_3\theta \quad (16)$$

$$\left(\frac{k_{nf}}{k_f}+\frac{4N}{3}\right)\frac{d^2\theta}{dy^2} - \phi_4 S\,Pr\frac{d\theta}{dy} = 0 \quad (17)$$

The boundary conditions are:

$$u = 1, \theta = 1 \quad at \quad y = 0$$
$$u = 0, \theta = 0 \quad at \quad y = 1 \quad (18)$$

Anaytical Solution:

Under the boundary conditions (18) the solution of equations (16-17) for non-dimensional velocity and temperature profile are represented as:

$$\theta = C_1 e^{sy} + C_2 \quad (19)$$

$$u = e^{a_4 y}[C_3\,cosh(a_5 y) + C_4\,sinh(a_5 y)] + a_8 e^{sy} + a_9 \quad (20)$$

Where:

$$C_1 = \frac{1}{1-e^s}, C_2 = \frac{-e^s}{1-e^s}, C_3 = 1 - a_8 - a_9, C_4 = \frac{a_{11}}{sinh(a_5)}$$

$$a = \frac{k_{nf}}{k_f} + \frac{4N}{3}, \quad b = \phi_4 S\,Pr, \; s = \frac{b}{a}, \; a_1 = S\phi_1\phi_2, \; a_2 = \phi_1 M^2 + \frac{1}{K}, \; a_3 = Gr\phi_1\phi_3,$$

$$a_4 = \frac{a_1}{2}, \; a_5 = \frac{\sqrt{a_1^2 + 4a_2}}{2}, \; a_6 = -a_3 C_1 A^2, \; a_7 = B^2 - a_1 BA - a_2 A^2, \; a_8 = \frac{a_6}{a_7},$$

$$a_9 = \frac{a_3 C_2}{a_2}, \; a_{10} = -a_8 e^s - a_9, \; a_{11} = \frac{a_{10}}{e^{a_4}} - C_3\, cosh(a_5)$$

RESULTS AND DISCUSSION

The effects on velocity and temperature distributions by several parameters have been portrayed in Figs. 2 to 10. The following parameters contains M (magnetic field parameter), K (permeability parameter), N (radiation parameter),ϕ (volume fraction of nanoparticles), Gr (Grashof number), and S (suction parameter) for steady & unsteady problems. In this case, the Prandtl number of the base fluid (water) is held constant at 6.2. $S = +0.5\ (i.e., S > 0)$ denotes injection at the plate at $y' = 0$ and simultaneous suction at $y' = H$, whereas $S = -0.5\ (i.e., S < 0)$ refers to suction at the plate $y' = 0$ and simultaneous injection at $y' = H$. When $\phi = 0$, the model reverts to the governing equations for a normal viscous fluid, thus eliminating any nanoscale characteristics.

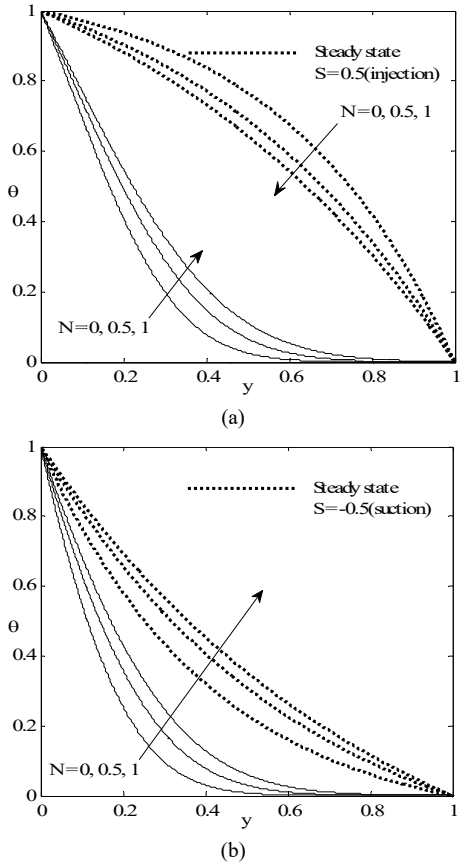

Fig. 2 Impact of variation in radiation parameter N in (a) Injection (S> 0) (b) Suction (S< 0) on the θ (temperature profile) when Pr = 6.2, time t = 0.1, ϕ = 0.1

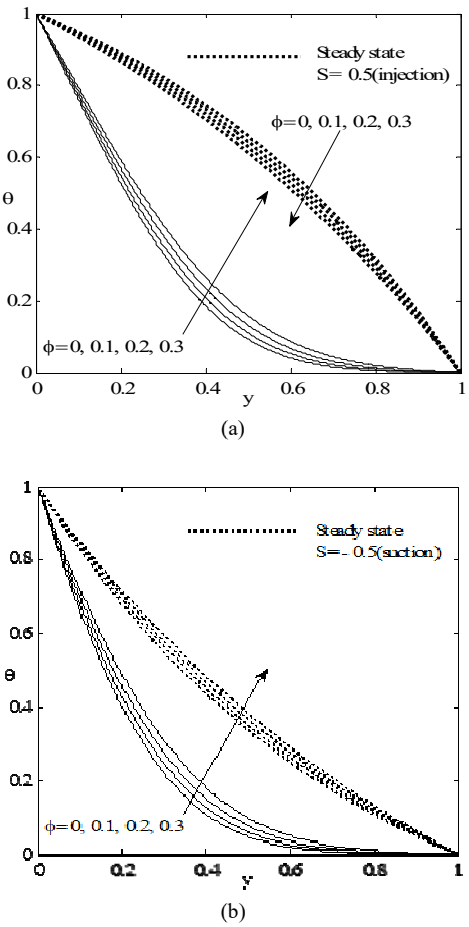

Fig. 3 Impact of variation in ϕ (volume fraction of nanoparticles) (a) Injection (S> 0) (b) Suction (S< 0) on θ (temperature profile) when Pr = 6.2, time t = 0.1, N=1.

The aforementioned composite figures depict temperature distribution of nanofluid flow due to N (radiation parameter) &ϕ (volume fraction) under suction/injection at the moving plate. It is noted that the temperature increases with an increase in N or ϕ during suction/injection in the unsteady case and during suction in the steady case since the increase in radiation parameter leads to an increase in fluid heating, enhancing temperature and thermal boundary layer thickness; however, injection at the moving plate for $S > 0$ in steady conditions leads to decreased temperature with an increase in N or ϕ.

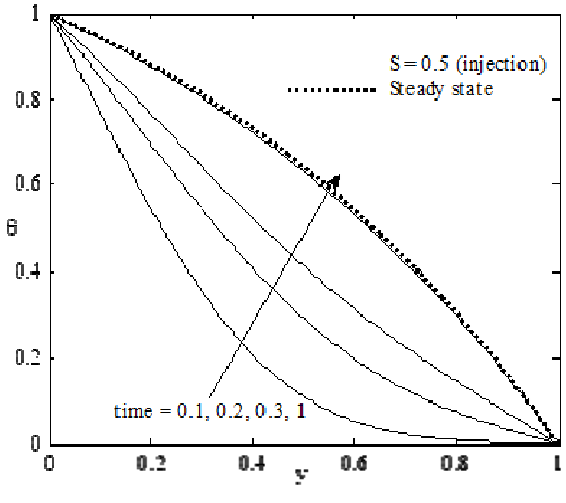

(a)

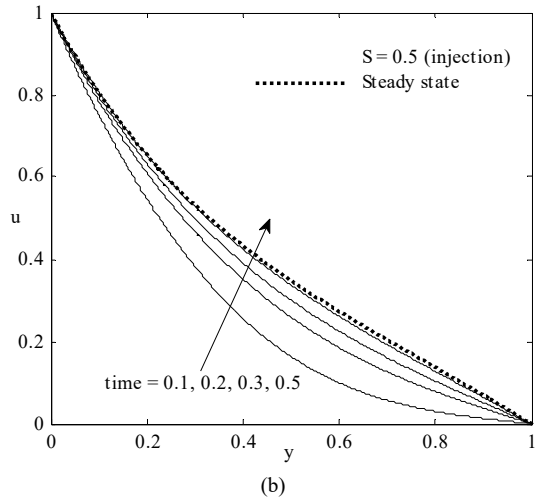

Fig. 4 Impact of variation in time t (a) Injection (S> 0) (b) Suction (S< 0) on the θ (temperature profile) when Pr = 6.2, N =1, ϕ = 0.1

The influence of dimensionless time t on θ (temperature profile) and f' (velocity profiles) are illustrated in Figs. (4-5) for injection as well for suction at $y = 0$. It is found that both the temperature & velocity of the field increase with time until it reaches a steady state. Furthermore, temperature variation in Fig. 4 shows an evident effect of t, in such a way that, in both cases at $y = 0$ injection dominates over suction

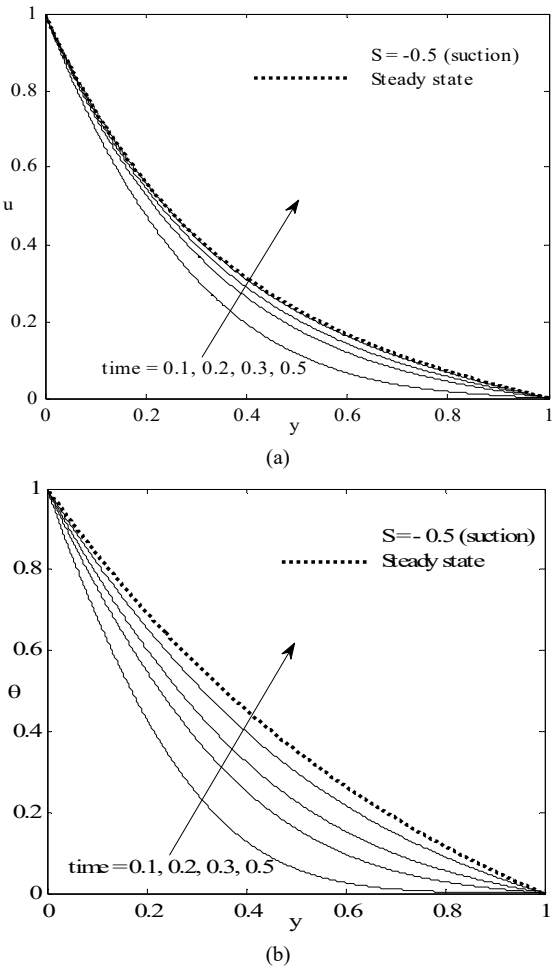

Fig. 5 Impact of variation in time t (a) Injection (S> 0) (b) Suction (S< 0) on the velocity profile when Pr = 6.2, ϕ = 0.1, M = 1, K = 0.1, Gr = 5, N =1

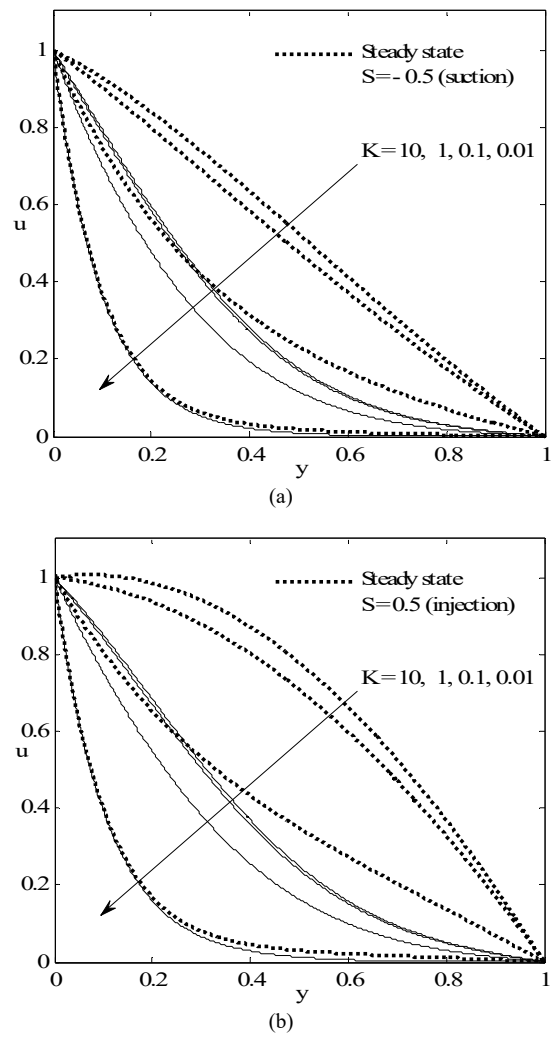

Fig. 6. Effect of variation in permeability parameter K (a) Injection (S> 0) (b) Suction (S< 0) on the velocity profile when Pr = 6.2, ϕ = 0.1, M = 1, t = 0.1, Gr = 5, N = 1

From Fig. So, in Fig 6(a-b) it is observed the significant influence of K on the steady state velocity when the injection or the suction is applied at $y = 0$. Velocity is increasing for more increment in permeability parameter but this increment is insignificant for higher permeability. It is because Darcy's resistance force is reduced by the increase of permeability, so the flow increases.

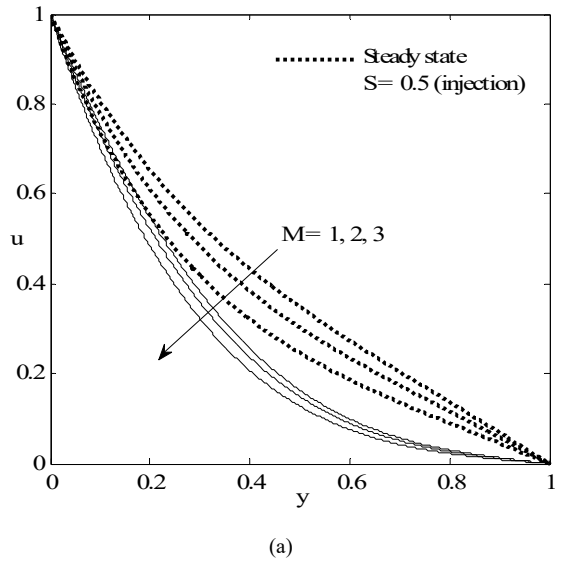

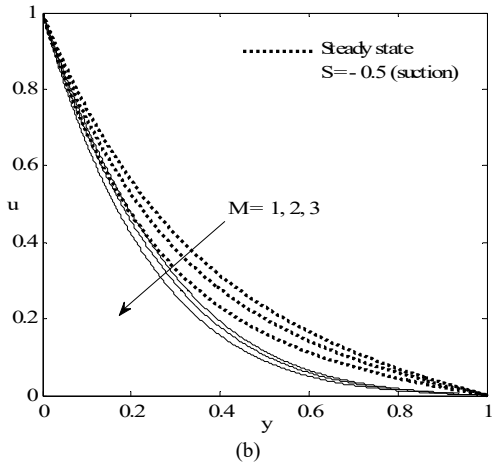

(b)

Fig. 7 Impact of variation in magnetic parameter M (a) Injection (S> 0) (b) Suction (S< 0) on the velocity profile when Pr = 6.2, ϕ = 0.1, K = 0.1, t = 0.1, Gr = 5, N = 1

Fig. shows that transient and steady state velocity of nanofluid decreases as magnetic field parameter M increases. Case 7(a-b) $S > 0$ and $S < 0$ in both cases. This is due to the activation of the Lorentz force when a magnetic field is present, the same that opposes the flow if the magnetic field is perpendicular to the flow direction.

In Fig. 8 (a-b), the influence of the volume fraction parameter ϕ on velocity distribution for both steady and unsteady states is shown. The outcome reveals that the flow velocity decreases on increasing the volume fraction of the nanoparticles in both states, while the ϕ does not significantly affect the velocity of the unsteady state for either case when the injection is at moving plate and suction at stationary plate or vice versa.

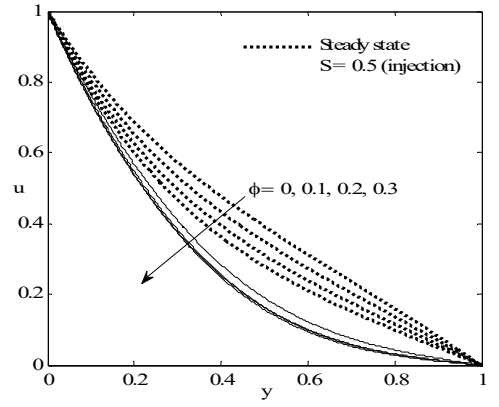

(a)

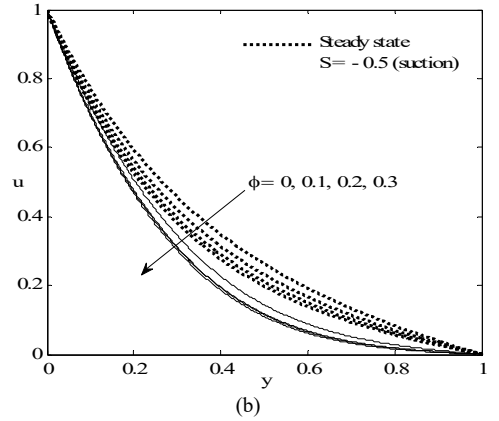

(b)

Fig. 8 Effect of variation in volume fraction of nanofluid ϕ (a) Injection (S> 0) (b) Suction (S<0) on the velocity profile when Pr = 6.2, M = 1, K = 0.1, t = 0.1, Gr = 5, N = 1

The impact of the Grashof number Gr on the velocity profile distribution w. r. to injection and suction is presented in Fig. 9 (a-b). For both cases, an increase in Gr causes an increase in both the steady and the unsteady velocities. Also, the effect of Gr is much more pronounced in the steady case than in the transient one in both Figs. 9 (a and b). In Fig. 10 (a-b), it is observed that in both the steady and unsteady states, velocity decreases with an increasein the radiation parameter for $S > 0$ (injection) at $y = 0$, whereas the opposite effect is observed for $S < 0$ (suction) at $y = 0$.

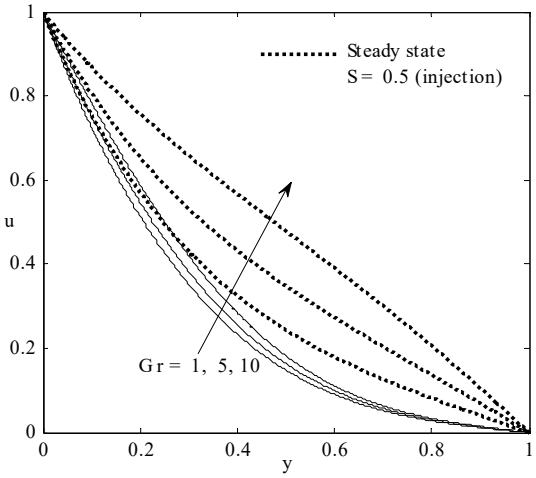

(a)

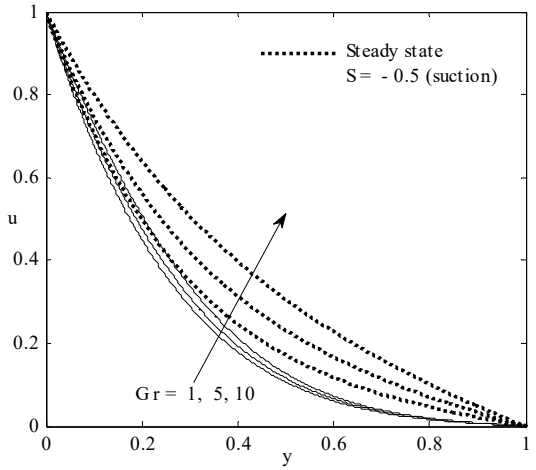

(b)

Fig. 9 Effect of variation in Grashoff number Gr (a) Injection (S> 0) (b) Suction (S< 0) on the velocity profile when Pr = 6.2, ϕ = 0.1, K = 0.1, t = 0.1, M = 1, N = 1

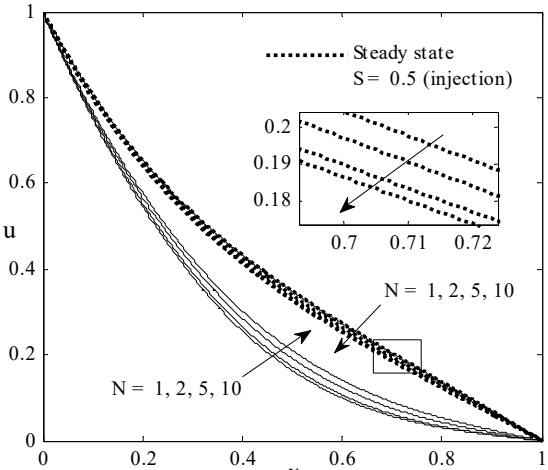

(a)

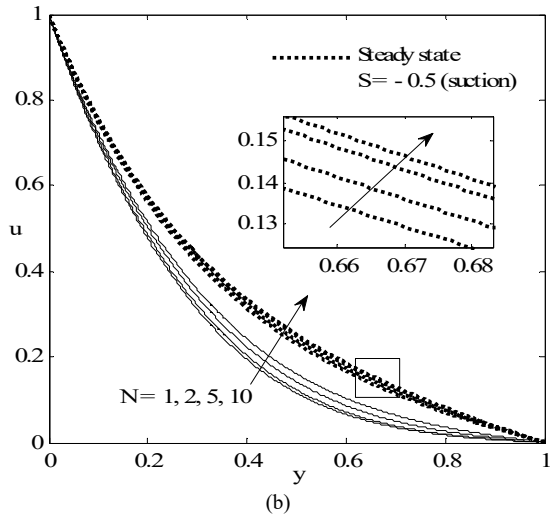

Fig. 10. Effect of variation in radiation parameter N (a) Injection (*S*> 0) (b) Suction (*S*< 0) on the velocity profile when Pr = 6.2, ϕ = 0.1, K = 0.1, t = 0.1, M = 1, Gr = 5

Conclusion

We analyse thermal radiation and suction/injection effects in a porous medium on free MHD convection Couette flow of a nanofluid in a permeable channel which is vertical. We study steady and unsteady flow & heat transferee under the same boundary conditions. We arrive at the conclusion that:

- For both situations' suction/injection, field velocity profile and temperature profile both shows hike with an increase in time until the steady state is attained.
- For both suction/injection, velocity profile shows hike with amplify effect of K (permeability parameter)&Gr (Grashof number) while reverse effect shows with increase of magnetic parameter M and volume fraction parameter φ.

With suction the temperature has increases with increase in effect of radiation and volume fraction for both steady and unsteady conditions but for injection, temperature increases in unsteady state whereas in steady state, it decreases.

Nomenclature

B_0 = Transverse magnetic field
q_r = Radiation of intensity
t' = time
u' = velocity of fluid in y' direction
g = gravitational acceleration
T' = dimensional temperature of fluid
σ = electrical conductivity of fluid
k_0 = permeability coefficient
μ_{nf} = Effective dynamic viscosity $\left[\mu_{nf} = \frac{\mu_f}{(1-\phi)^{2.5}}\right]$
ρ_{nf} = effective density $\left[\rho_{nf} = (1-\phi)\rho_f + \phi\rho_s\right]$
ν_{nf} = effective kinematic viscosity $\left[\nu_{nf} = \frac{\mu_{nf}}{\rho_{nf}}\right]$,
k_{nf} = thermal conductivity $\left[\frac{k_{nf}}{k_f} = \frac{(k_s+(n-1)k_f)-\phi(n-1)(k_f-k_s)}{(k_s+(n-1)k_f)+\phi(k_f-k_s)}\right]$
β_{nf} = thermal expansion $\left[(\rho\beta)_{nf} = (1-\phi)(\rho\beta)_f + \phi(\rho\beta)_s\right]$
$\left(\rho C_p\right)_{nf}$ = heat capacitance of the nanofluid $\left[\left(\rho C_p\right)_{nf} = (1-\phi)\left(\rho C_p\right)_f + \phi\left(\rho C_p\right)_s\right]$
ϕ = solid volume fraction of nanofluid
ρ_f = reference density
μ_f = dynamic viscosity
k_f = thermal conductivity
β_f = thermal expansion
$\left(\rho C_p\right)_f$ = heat capacitance of base fluid
ρ_s = reference density of solid
μ_s = dynamic viscosity of solid
k_s = thermal conductivity of solid
β_s = electrical conductivity of solid
$\left(\rho C_p\right)_s$ = heat capacitance of solid
nf, f, s = nanofluid, base fluid, solid nanoparticle
σ_1 = Stefan–Boltzmann constant
k_1 = mean absorption coefficient
u = velocity
θ = temperature
$M^2 = \frac{\sigma B_0^2 H^2}{\rho_f \nu_f}$ = magnetic parameter
$Pr = \frac{k_f}{(\nu\rho C_p)_f}$ = Prandtl number
$S = \frac{V_0 H}{\nu_f}$ = suction/injection parameter
$Gr = \frac{g\beta_f H^2 (T_w - T_0)}{U\nu_f}$ = Grashoff number
$N = \frac{4\sigma_1 T_0^3}{k_1 k_f}$ = radiation parameter
$K = \frac{k_0}{H^2}$ = porosity parameter

Conflicts of interest

Corresponding authors declared that there have no conflicts of interest.

Acknowledgments

The authors gratefully acknowledge the respective institutions for making resources and support available to enable undertaking this research work. They also acknowledge the constructive engagement and encouragement from their colleagues and peers that has added to this work. The study did not receive any funding.

REFERENCES

1. Kumar J. P., J. C. Umavathi, A. J. Chamkha, and I. Pop, "Fully-developed free-convective flow of micropolar and viscous fluids in a vertical channel," *Applied Mathematical Modelling*, vol. 34, no. 5, pp. 1175–1186, May 2010, doi: 10.1016/j.apm.2009.08.007.
2. Umavathi J. C., J. P. Kumar, A. J. Chamkha, and I. Pop, "Mixed Convection in a Vertical Porous Channel," *Transp Porous Med*, vol. 61, no. 3, pp. 315–335, Dec. 2005, doi: 10.1007/s11242-005-0260-5.
3. Hussanan A., M. Z. Salleh, R. M. Tahar, and I. Khan, "Unsteady Boundary Layer Flow and Heat Transfer of a Casson Fluid past an Oscillating Vertical Plate with Newtonian Heating," *PLOS ONE*, vol. 9, no. 10, p. e108763, Oct. 2014, doi: 10.1371/journal.pone.0108763.
4. Khalid A., I. Khan, A. Khan, and S. Shafie, "Unsteady MHD free convection flow of Casson fluid past over an oscillating vertical plate embedded in a porous medium," *Engineering Science and Technology, an International Journal*, vol. 18, no. 3, pp. 309–317, Sep. 2015, doi: 10.1016/j.jestch.2014.12.006.

5. Khem C., K. Rakesh, and S. Shavnam, "Hydromagnetic oscillatory vertical Couette flow of radiating fluid through porous medium with slip and jump boundary conditions," *Int. J. Phys. Math. Sci.*, vol. 3, no. 1, pp. 82–90, 2012.
6. Jha B., A. K. Singh, and H. S. Takhar, "Transient free-convective flow in a vertical channel due to symmetric heating," *International journal of applied mechanics and engineering*, vol. 8, no. 3, pp. 497–502, 2003.
7. Jha B. K., A. K. Samaila, and A. O. Ajibade, "Unsteady Natural Convection Couette Flow of a Reactive Viscous Fluid in a Vertical Channel," *Comput Math Model*, vol. 24, no. 3, pp. 432–442, Jul. 2013, doi: 10.1007/s10598-013-9188-8.
8. Kataria H. R.and H. R. Patel, "Radiation and chemical reaction effects on MHD Casson fluid flow past an oscillating vertical plate embedded in porous medium," *Alexandria Engineering Journal*, vol. 55, no. 1, pp. 583–595, Mar. 2016, doi: 10.1016/j.aej.2016.01.019.
9. Kataria H. R.and H. R. Patel, "Soret and heat generation effects on MHD Casson fluid flow past an oscillating vertical plate embedded through porous medium," *Alexandria Engineering Journal*, vol. 55, no. 3, pp. 2125–2137, Sep. 2016, doi: 10.1016/j.aej.2016.06.024.
10. Attia, H. A. "The effect of suction and injection on unsteady couette flow with variable properties," *Kragujevac J. Sci*, vol. 32, pp. 17–24, 2010.
11. Rundora L. and O. D. Makinde, "Effects of suction/injection on unsteady reactive variable viscosity non-Newtonian fluid flow in a channel filled with porous medium and convective boundary conditions," *Journal of Petroleum Science and Engineering*, vol. 108, pp. 328–335, Aug. 2013, doi: 10.1016/j.petrol.2013.05.010.
12. Jha B. K., B. Y. Isah, and I. J. Uwanta, "Unsteady MHD free convective Couette flow between vertical porous plates with thermal radiation," *Journal of King Saud University - Science*, vol. 27, no. 4, pp. 338–348, Oct. 2015, doi: 10.1016/j.jksus.2015.06.005.
13. Jha B. K., B. Y. Isah, and I. J. Uwanta, "Combined effect of suction/injection on MHD free-convection flow in a vertical channel with thermal radiation," *Ain Shams Engineering Journal*, vol. 9, no. 4, pp. 1069–1088, Dec. 2018, doi: 10.1016/j.asej.2016.06.001.
14. Maxwell J. C., *A Treatise on Electricity and Magnetism*. Clarendon Press, 1873.
15. Choi S. U. S. and J. A. Eastman, "Enhancing thermal conductivity of fluids with nanoparticles," Argonne National Lab. (ANL), Argonne, IL (United States), ANL/MSD/CP-84938; CONF-951135-29, Oct. 1995. Accessed: May 25, 2025. [Online]. Available: https://www.osti.gov/biblio/196525
16. Buddakkagari V. and M. Kumar, "Transient Boundary Layer Laminar Free Convective Flow of a Nanofluid Over a Vertical Cone/Plate," *Int. J. Appl. Comput. Math*, vol. 1, no. 3, pp. 427–448, Sep. 2015, doi: 10.1007/s40819-015-0027-9.
17. Chauha D. S. and V. Kumar, "Radiation Effects on Unsteady Flow through a Porous Medium Channel with Velocity and Temperature Slip Boundary Conditions".
18. Baoku I. G., C. Israel-Cookey, and B. I. Olajuwon, "Magnetic field and thermal radiation effects on steady hydromagnetic couette flow through a porous channel," *Surveys in Mathematics and its Applications*, vol. 5, pp. 215–228, 2010.
19. Chauhan D. S.and P. Rastogi, "Heat Transfer Effects on Rotating MHD Couette Flow in a Channel Partially Filled by a Porous Medium with Hall Current," *Journal of Applied Science and Engineering*, vol. 15, no. 3, pp. 281–290, Sep. 2012, doi: 10.6180/jase.2012.15.3.09.
20. Chauhan S. and V. Kumar, "Heat transfer effects in a Couette flow through a composite channel partly filled by a porous medium with a transverse sinusoidal injection velocity and heat source," *Therm sci*, vol. 15, no. suppl. 2, pp. 175–186, 2011, doi: 10.2298/TSCI100716055C.
21. Jain S., V. Kumar, and S. Bohra, "Entropy Generation in Generalized Couette Flow through Porous Medium with Different Thermal Boundary Conditions," *International Journal of Energy & Technology*, vol. 7, pp. 40–48, 2015.
22. Ibrahim W.and B. Shanker, "Boundary-Layer Flow and Heat Transfer of Nanofluid Over a Vertical Plate With Convective Surface Boundary Condition," *Journal of Fluids Engineering*, vol. 134, no. 8, p. 081203, Aug. 2012, doi: 10.1115/1.4007075.
23. Kumari M. and R. S. R. Gorla, "Mixed Convective Boundary Layer Flow Over a Vertical Plate Embedded in a Porous Medium Saturated with a Nanofluid," *J Nanofluids*, vol. 1, no. 2, pp. 166–174, Dec. 2012, doi: 10.1166/jon.2012.1019.
24. Raju C. S. K., M. J. Babu, N. Sandeep, V. Sugunamma, and J. V. R. Reddy, "Radiation and Soret Effects of MHD Nanofluid Flow over a Moving Vertical Moving Plate in Porous Medium," *Chemical and Process Engineering Research www.iiste.org*, vol. 30, pp. 9–23, 2015.
25. Krishna P. M., V. Sugunamma, and N. Sandeep, "Radiation and magnetic field effects on unsteady natural convection flow of a nanofluid past an infinite vertical plate with heat source," *Chem Process Eng Res*, vol. 25, pp. 39–52, 2014.
26. Rajesh V., M. P. Mallesh, and O. A. Bég, "Transient MHD free Convection Flow and Heat Transfer of Nanofluid Past an Impulsively Started Vertical Porous Plate in the Presence of Viscous Dissipation," *Procedia Materials Science*, vol. 10, pp. 80–89, Jan. 2015, doi: 10.1016/j.mspro.2015.06.028.
27. Gorla R. S. R. and A. Chamkha, "Natural Convective Boundary Layer Flow Over a Nonisothermal Vertical Plate Embedded in a Porous Medium Saturated With a Nanofluid," *Nanoscale and Microscale Thermophysical Engineering*, vol. 15, no. 2, pp. 81–94, Apr. 2011, doi: 10.1080/15567265.2010.549931.
28. Jain S.and S. Bohra, "Radiation Effects in Flow through Porous Medium over a Rotating Disk with Variable Fluid Properties," *Advances in Mathematical Physics*, vol. 2016, pp. 1–12, 2016, doi: 10.1155/2016/9671513.
29. Elsaid E. M.and M. S. Abdel-wahed, "Mixed convection hybrid-nanofluid in a vertical channel under the effect of thermal radiative flux," *Case Studies in Thermal Engineering*, vol. 25, p. 100913, Jun. 2021, doi: 10.1016/j.csite.2021.100913.
30. Alizadeh R., N. Karimi, R. Arjmandzadeh, and A. Mehdizadeh, "Mixed convection and thermodynamic irreversibilities in MHD nanofluid stagnation-point flows over a cylinder embedded in porous media," *J Therm Anal Calorim*, vol. 135, no. 1, pp. 489–506, Jan. 2019, doi: 10.1007/s10973-018-7071-8.
31. Waqas H., S. M. Raza Shah Naqvi, M. S. Alqarni, and T. Muhammad, "Thermal transport in magnetized flow of hybrid nanofluids over a vertical stretching cylinder," *Case Studies in Thermal Engineering*, vol. 27, p. 101219, Oct. 2021, doi: 10.1016/j.csite.2021.101219.

32. Salahuddin T., N. Siddique, M. Khan, and Y. Chu, "A hybrid nanofluid flow near a highly magnetized heated wavy cylinder," *Alexandria Engineering Journal*, vol. 61, no. 2, pp. 1297–1308, Feb. 2022, doi: 10.1016/j.aej.2021.06.014.
33. Kumar Mishra N., K. Abdulkhaliq M. Alharbi, K. Ur Rahman, Adnan, S. M. Eldin, and M. Z. Bani-Fwaz, "Investigation of improved heat transport featuring in dissipative ternary nanofluid over a stretched wavy cylinder under thermal slip," *Case Studies in Thermal Engineering*, vol. 48, p. 103130, Aug. 2023, doi: 10.1016/j.csite.2023.103130.
34. Makhdoum B. M., Z. Mahmood, U. Khan, B. M. Fadhl, I. Khan, and S. M. Eldin, "RETRACTED: Impact of suction with nanoparticles aggregation and joule heating on unsteady MHD stagnation point flow of nanofluids over horizontal cylinder," *Heliyon*, vol. 9, no. 4, p. e15012, Apr. 2023, doi: 10.1016/j.heliyon.2023.e15012.
35. Nabwey H. A., A. M. A. EL-Hakiem, W. A. Khan, Z. M. Abdelrahman, A. M. Rashad, and M. A. Hawsah, "Magnetic williamson hybrid nanofluid flow around an inclined stretching cylinder with joule heating in a porous medium," *Chemical Engineering Journal Advances*, vol. 18, p. 100604, May 2024, doi: 10.1016/j.ceja.2024.100604.
36. Ali F., A. Zaib, M. Abbas, G. Anitha, K. Loganathan, and G. R. Reddy, "Radiative flow of cross ternary hybrid nanofluid (MoS TiO, Ag/CMC-water) in a Darcy Forchheimer porous medium over a stretching cylinder with entropy minimization," *Heliyon*, vol. 10, no. 14, p. e34048, Jul. 2024, doi: 10.1016/j.heliyon.2024.e34048.
37. Sohail M., K. Ilyas, E. Rafique, and S. Jahan, "OHAM Analysis of Bio-Convective Flow of Oldroyd-B nanofluid under Thermal Radiation Impact Past over a Stretching Sheet," *Scientia Iranica*, vol. 0, no. 0, pp. 1–33, Feb. 2025, doi: 10.24200/sci.2025.63873.8635.

****